Materials and Structures / Matériaux et Constructions, Vol. **36**, April 2003, pp 191-196

On the use of nanoindentation for cementitious materials

G. Constantinides, F.-J. Ulm and K. Van Vliet
Massachusetts Institute of Technology, Cambridge, MA 02139, USA

ABSTRACT

Recent progress in experimental and theoretical nanomechanics opens new venues in materials science for the nano-engineering of cement-based composites. In particular, as new experimental techniques such as nanoindentation provide unprecedented access to micro-mechanical properties of materials, it becomes possible to identify the mechanical effects of the elementary chemical components of cement-based materials at the scale where physical chemistry meets mechanics, including the properties of the four clinker phases, of portlandite, and of the C-S-H gel. In this paper, we review some recent results obtained by nanoindentation, which reveal that the C-S-H gel exists "mechanically" in two different forms, a low-density form and a high-density form, which have different mean stiffness and hardness values and different volume fractions. While the volume fractions of the two phases depend on mix proportions, the mean stiffness and hardness values do not change from one cement-based material to another; instead they are intrinsic properties of the C-S-H gel.

RÉSUMÉ

Les récents progrès en "nanomécanique", aussi bien sur le plan théorique qu'expérimental, ouvrent de nouvelles perspectives en science des matériaux pour la nano-ingénierie des composites à base de ciment. Grace à de nouvelles techniques expérimentales telles que la 'nanoindentation', qui permet d'avoir un accès sans précédent aux propriétés micromécaniques des matériaux, il devient notamment possible d'identifier les effets mécaniques des composants chimiques élémentaires à l'échelle où la chimie rejoint la mécanique; cela inclut les propriétés des quatre phases de clinkers, de la portlandite et du gel de C-S-H. Dans le présent article, nous analysons quelques résultats récents obtenus par nanoindentation; ces résultats révèlent que le gel de C-S-H existe "mécaniquement" sous deux formes différentes, l'une à faible densité et l'autre à forte densité. La valeur moyenne du module d'élasticité, de la dureté, ainsi que la fraction volumique de ces deux formes sont différentes. Alors que la fraction volumique des deux phases dépend de la formulation du mélange, les valeurs moyennes du module d'élasticité et de la dureté sont identiques d'un composite à l'autre ; il s'agit de propriétés intrinsèques du gel de C-S-H.

1. INTRODUCTION

Concrete, like many other materials (whether man-made, geological or biological), exhibit heterogeneous features over a wide range of length scales, from the nanoscale of the elementary chemical components to the macroscopic scale of the aggregate-mortar composite. This multi-scale heterogeneity ultimately determines the *in vivo* mechanical performance (stiffness, strength), and degradation (damage, fracture, failure) of cementitious materials. While most codes of practice in concrete engineering account for this heterogeneity through probability theory to achieve certain macroscopic material properties with some certainty, current trends in concrete science and engineering aim at a better representation of this heterogeneity at multiple length scales, to ultimately identify the scale where physical chemistry meets mechanics. The rationale behind this approach is that the different chemical components of cement-based materials are defined by specific chemical

Editorial Note
Prof. Franz-Josef Ulm is a RILEM Senior Member. He was awarded the 2002 Robert L'Hermite Medal. He is Associate Editor for Concrete Science and Engineering.

equilibrium states, for which the probability that some solid chemical compounds go into the solution is smaller than the probability that the same chemical species in the solution precipitates onto the solid. Such an equilibrium state is associated with a stable material state. Hence, if it were possible to break down the heterogeneities of cement-based materials to this scale, where the solid material manifests itself in a chemically stable state, and to assess, at this scale, the mechanical material properties, it would be possible to translate with high confidence chemical equilibrium states into macroscopic material properties. The expected outcome of such an endeavor is a blueprint of the elementary chemomechanical components of cementitious materials, which do neither change in time, nor from one cementitious material to another.

This paper reviews results of ongoing research on the use and role of instrumented nanoindentation towards the aim of identifying the scale where cement chemistry meets mechanics.

2. INSTRUMENTED INDENTATION

It has long been hypothesized that the localized contact response measured by an instrumented indentation experiment can serve to characterize the mechanical properties of materials as quantitatively as conventional testing techniques such as uniaxial compression and tension. This experimental approach provides a continuous record of the variation of the depth of penetration, h, as a function of imposed indentation load, P, into the indented specimen surface. Advances in hardware and software control currently enable maximum penetration depths on the nanometer scale, such that nanoscale instrumented indentation provides a convenient, non-destructive means to evaluate the basic mechanical response of small material volumes of a bulk, thin film, or composite materials. Commercially available indenters accommodate various indenter geometries, including sharp pyramidal, conical or spherical probes, such elastic and plastic mechanical properties can be estimated at any scale within the limits defined by the indenter dimensions and maximum penetration depth. Thus, instrumented indentation is a versatile tool for material characterization, particularly at scales where classical mechanical tests based on volume-averaged stresses are inadequate.

2.1 Historical background

The application of indentation methods to assess material properties can be traced back to the work of the Swedish engineer Brinell. Pushing a small ball of hardened steel or tungsten carbide against the surface of the specimen, Brinell empirically correlated the shape of the resulting, permanent impression (indentation) with the strength of metal alloys. The first accessible work of this pioneering approach of the Swedish engineer can be found in a 1900 International congress in Paris [1]. The merits of Brinell's proposal were quickly appreciated by contemporaries: Meyer (1908), O'Neill (1944) and Tabor (1951) [2] suggested empirical relations to transform indentation data into meaningful mechanical properties.

The indentation test provides a $P - h$ curve, and the extraction of material properties requires an inverse analysis of these data. The theoretical foundation of elastic indentation is set by Boussinesq's problem and the Hertz contact problem: Boussinesq's stress and displacement solution of an elastic half-space loaded by a rigid, axisymmetric indenter [3], which was subsequently extended for conical and cylindrical indenter geometry, provides a linear $P - h$ relation. Hertz's elastic contact solution [4] of two spherical surfaces with different radii and elastic constants provides a means of evaluating the contact area of indentation, and forms the basis of much experimental and theoretical work in indentation analysis based on contact mechanics. Subsequently, Sneddon [5] derived general relationships among load, displacement and contact area for any indenter describable as a solid of revolution.

Incorporating plasticity phenomena in the indentation analysis is a much more complex problem. The nonlinear nature of the constitutive relations, as well as the increased number of material properties required to describe material behavior, complicate the derivation of analytical solutions. As a result, much of our knowledge of the importance of plasticity in indenter contact problems has been derived through experimentation, and more recently through finite element simulations. Various researchers have proposed semi-analytical procedures by which the experimental $P - h$ response can be used to calculate elastic properties such as the elastic modulus E, pseudo-properties characterizing resistance to deformation such as hardness H, and plastic properties such as yield stress σ_y and strain hardening exponent n [6-9]. Experimental data has demonstrated that analysis of indentation data via elastic solutions provides reasonable estimates of the elastic modulus and hardness of the indented material, provided that the contact area is measured or calculated accurately.

2.2 Indentation analysis of elastic modulus

A typical indentation test is composed of a loading and an unloading response (Fig. 1). The slope of the unloading curve can be used as a measure of the elastic properties of the material. The behavior of the material during unloading is assumed purely elastic, in which case elastic punch theory can be employed to determine the elastic properties. For a linear isotropic elastic material, use of the elastic solution for a flat cylindrical punch relating the applied

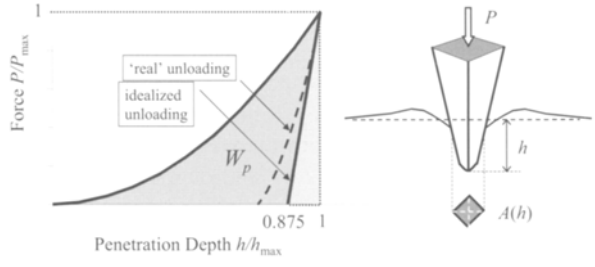

Fig. 1 - Principle of indentation test: Left – P - h curve [8]; Right – True projected contact surface in the case of sink-in below Vickers indenter.

force, P, with the indentation depth, h, yields the following expression for the initial unloading response dP/dh:

$$\frac{dP}{dh} = c^* A^{1/2} E^* \tag{1}$$

where $c^* = 2/\sqrt{\pi}$, A is the contact area, and E^* is given by:

$$\frac{1}{E^*} = \frac{1-\nu^2}{E} + \frac{1-\nu_{in}^2}{E_{in}} \tag{2}$$

where E, ν and E_{in}, ν_{in} are the elastic constants of the indented material and the indenter, respectively. For the diamond indenter used in the present experiments, the elastic properties (E_{in}=1000 GPa, ν_{in}=0.07) are at least one order of magnitude greater than most cementitious constituents, so that $E^* \approx E / (1-\nu^2)$. In this case, E can be determined from the measured slope at the onset of unloading, provided that a reasonable estimate of the Poisson's ratio[1] and an independent measure of the contact area A upon unloading are available. Equation (1) is based on the elastic solution for flat-ended cylindrical punch, but holds for any punch that can be described by a smooth solid of revolution (spherical, conical, elliptical etc.) [7]. Berkovich and Vickers indenters (four- and three-sided pyramidal cones, respectively), which are more commonly applied in instrumented indentation techniques, cannot be described as bodies of revolution. However, it has been found experimentally and by means of finite element simulations that the deviation from relation (1) of pyramidal and other geometrical shapes during unloading is negligible [10, 7, 9]. The constant $c^* = 1.142$ for the Vickers pyramid indenter (square cross section), and $c^* = 1.167$ for the Berkovich indenter (triangular cross section) differ little from $c^* = 2/\sqrt{\pi} = 1.1284$ of the flat cylindrical indenter. In other words, relation (1) can be used without large error, even when the indenter is not a true body of revolution; that is it can be considered as a general characteristic of elastic indentation mechanics.

The key to accurate estimation of the elastic properties is accurate identification of the true maximum contact area A_{max} at maximum indentation load P_{max}. For a flat indenter, A coincides with the circular cylinder cross-section. Historically, A represents the projected contact area. The determination of the true contact area requires consideration of pile-up or sink-in phenomena that occur during loading as a consequence of plastic deformation. These phenomena have received some attention in recent years [11-13], and led to the development of unique correlations between penetration depth h and true contact area A for commercially available sharp indenters [8, 9]. This method circumvents the need for contact area measurement through visual observations while, at the same time, taking into account material pile-up and sink-in at the indentation perimeter. These developments provide a means of determining the elastic modulus directly from the sharp $P - h$ response obtained during the complete loading/unloading cycle:

$$E^* = d^* \frac{H}{1 - W_p / W_t} \tag{3}$$

where $d^* = 5$ for the Vickers pyramid indenter and $d^* = 4.678$ for the Berkovich indenter; $H = P/A\ (h)$ is the average pressure under the indenter; $W_t = \int_0^h P(s)ds$ is the total work done by the indenter in deforming the material; and W_p is the plastic work. These quantities are extracted from the $P - h$ curve, as sketched in Fig. 1. In practical applications, E is determined with the help of (1) or (3) for the maximum load P_{max} and penetration depth h_{max}, that are associated with a specific material scale under consideration. As a rough estimate, the effective material length scale of the bulk material under investigation in an indentation test operated to penetration depth h_{max} is $\ell \approx 4 \times h_{max}$.

2.3 Indentation analysis of hardness measurements

Within the context of continuum analyses, sharp pyramidal or conical indenters lead to geometrically similar indentation states. That is, for a given indenter shape or included tip angle, the average pressure below the indenter, P/A, is independent of the indentation load P or the true contact area A (*e.g.* [8]). This average contact pressure is proportional to the historic definition of hardness H. Theoretically, H can be determined at any point along the $P - h$ curve provided the true contact area is accounted for. In the same way as for the elastic stiffness, however, the hardness $H = P_{max}/A_{max}$ is determined for the maximum load P_{max} and penetration depth h_{max} associated with a specific material scale under investigation. In conventional micro-hardness tests the area of contact A_{max} is determined by measuring the diagonal lengths of the indentation after load removal. This estimate of the contact area involves the assumptions that the elastic recoveries during unloading are negligible, so that there is little change in geometry. This assumption is sound for certain, very soft metals, but has not been verified for pressure sensitive-frictional materials.

The assumption of negligible elastic recoveries during unloading is equivalent to the assumption that the elastic energy stored in the material system during loading to P_{max} is negligible compared to the plastic work; *i.e.* $1 - W_p/W_t \ll 1$. This may justify yield design approaches for the determination of the link between hardness and strength properties of the material[2]. For non-frictional isotropic materials which do not exhibit any appreciable strain hardening, application of yield design delivers a ratio of hardness-to-uniaxial yield strength of roughly $H/\sigma_0 \approx 2.7\text{-}3$, which holds for certain metals. This interpretation does not hold for frictional materials, for which hardness H is a function of more than one material parameter (*e.g.* cohesion c and friction angle φ; *i.e.* $H = H(c, \varphi)$), so that the

[1] *However, it is not necessary to know the value of the Poisson's ratio with great precision to obtain a good value of the elastic modulus.*

[2] *Recall that yield design assumes that the material system at plastic collapse has exhausted its capacity to store externally supplied work (here $dW_t = P(h)\,dh$) into recoverable (i.e., elastic) energy. At plastic collapse, the externally supplied work rate is entirely dissipated into heat formation (e.g., [24]).*

hardness-to-uniaxial strength ratio is a function of (at least) the friction angle, *i.e.*,

$$\frac{H}{\sigma_0} = F(\varphi) \qquad (4)$$

For cementitious materials, reported values for this ratio are some order of magnitude larger than typical values for metals, that is $H / \sigma_0 = 30\text{-}60$ [14], which highlights the effect of friction on the hardness H. Moreover, good yield design estimates for function $H / \sigma_0 = F(\varphi)$ are not available, complicating the assessment of the relation between hardness and strength properties of frictional materials.

2.4 Indentation analysis of heterogeneous materials

Indentation gives access to bulk properties of the indented material at a length scale of $\mathcal{L} \approx 4 \times h_{max}$, at which the material is considered as homogeneous. The continuum assumption which is at the basis of the elasticity and strength-hardness formulas requires in addition that the characteristic length scale of the representative elementary material volume (r.e.v.) satisfies $\ell << \mathcal{L}$. Hence, the material properties that are extracted from a $P - h$ curve are material properties of an r.e.v. averaged over a structural volume $\propto \mathcal{L}^3$.

Let us now consider that the material at a length $L >> \mathcal{L}$ is composed of a finite number n of homogeneous phases of characteristic length scale $\ell << \mathcal{L} << L$. If these phases are perfectly distributed, the probability of indenting on each phase is equal to the volume fraction the phase realizes in volume $\propto L^3$. That is, a large number of indentation tests does not only give access to the averaged material properties of the material at the length scale $\mathcal{L}$, but has also the potential to give access to the volume fractions; from:

$$f_i = \frac{N_i}{N}; \sum_{i=1}^{n} N_i = N \qquad (5)$$

where N_i is the number of indentations on material phase i, that can be identified by the difference in material properties; that is f_i is the volume fraction of a 'mechanically' identifiable material phase.

3. NANOINDENTATION ON CEMENTITIOUS MATERIALS

Indentation tests on cementitious materials have been reported by several authors, *i.e.*: 1) Igarashi *et al.* [14] used a Vickers indenter with a maximum penetration depth on the order of $h_{max} \approx 10^{-5}$ m, which gives access to the bulk properties of cement paste at a sub-millimeter to millimeter material length scale, 2) Zhu *et al.* [15-17] used instrumented indentation to study (in a qualitative manner) the mechanical properties of the interfacial transition zone in reinforced concrete, 3) Kholmyansky *et al.* [18] discusses the experimental methods for hardness determination on fine-grained concrete. To our knowledge, the first indentation results of individual constituents of Portland cement were provided by Velez *et al.* [19], and Acker [20]. The first reported nanoindentation results of the elastic modulus and hardness of the major clinker phases (C_2S, C_3S, C_3A, C_4AF)[3], and the second provided values for portlandite ($CH=Ca(OH)_2$) and the C-S-H gel for different C/S-ratio. These results were obtained on an ultra-high performance cementitious composite material, DUCTAL, using a Berkovich indenter with penetration depths of about $h_{max} \approx 0.3\text{-}0.5 \times 10^{-6}$ m. Thus, indentation responses corresponded to bulk properties of the different phases at a characteristic length scale in the micrometer range. Constantinides and Ulm [21, 22] confirmed the stiffness value for CH, and provided stiffness values of the two-types of C-S-H of an ordinary Portland cement paste prepared at a water-cement ratio of $w/c = 0.5$, in a non-degraded and an asymptotically leached state. The results were obtained with a NanoTest 200 Berkovich indenter via arrays of equally spaced nanoindentations at a fixed h_{max}.

3.1 Identification of the intrinsic stiffness of the two-types of C-S-H

Fig. 2a displays the results of the elastic nanoindentation tests on the C-S-H matrix of a non-degraded (*i.e.* hardened) $w/c = 0.5$ cement paste, and Fig. 2b displays the same results for the material after calcium leaching (using an

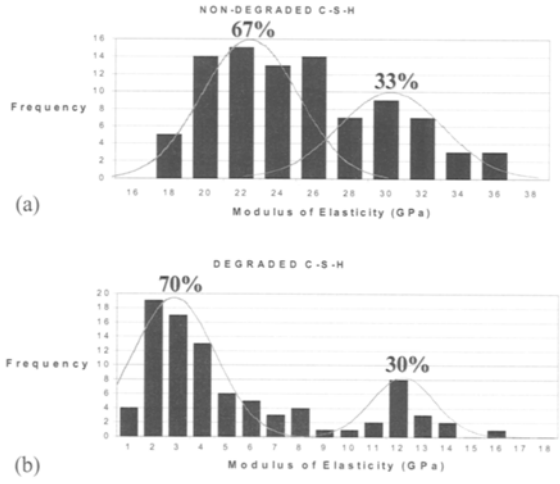

Fig. 2 - Histogram of (elastic) Nanoindentation results: (a) non-degraded C-S-H; (b) degraded C-S-H. Adopted from [21, 22].

ammonium nitrate solution described in details in [23]). A series of 200 indentations tests covering an area of roughly $L^2 = 1000\ \mu m^2$ (see Fig. 3) was conducted which represents roughly the distance in between large portlandite crystals in the considered cementitious material system. The maximum penetration depth in each test was $h_{max} \approx 0.3\text{-}0.5 \times 10^{-6}$m, which means that the properties that are obtained with this test are representative of a material at a length scale of $\mathcal{L} \approx 10^{-6}$ m.

[3] *The cement's chemistry abbreviation will be used in this paper ($C_3S = 3{\cdot}CaO{\cdot}SiO_2$, $C_2S = 2{\cdot}CaO{\cdot}SiO_2$, $C_3A = 3{\cdot}CaO{\cdot}Al_2O_3$, $C_4AF = 4{\cdot}CaO{\cdot}Al_2O_3{\cdot}Fe_2O_3$).*

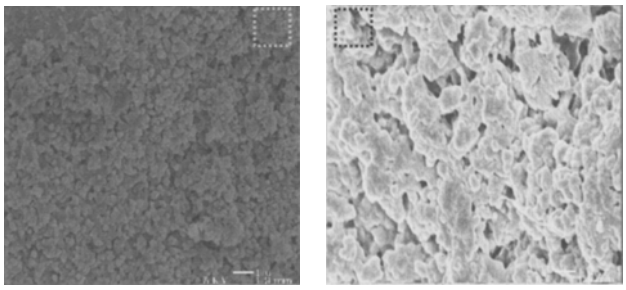

Fig. 3 - SEM images of C-S-H matrix (w/c = 0.5): Non-degraded (Left), calcium leached (Right). The boxes in these figures represent the effective influence zone affected by nanoindentation of a size of roughly 9 x h, where h is the penetration depth [22]. The scale bar indicates 1 μm. The distance and voltage used were 19 mm and 5kV respectively.

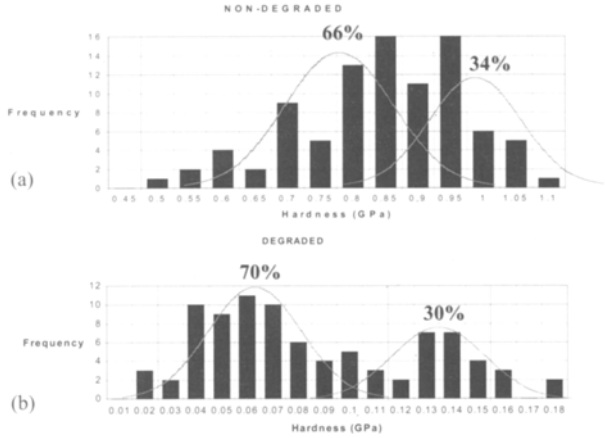

Fig. 4 - Histogram of hardness Nanoindentation results: (a) non-degraded C-S-H; (b) degraded C-S-H.

The results displayed in Fig. 2 are represented in the form of a stiffness histogram. The frequency distribution exhibits a clear bi-modal structure that can be associated with two types of C-S-H, characterized by two different E-moduli, and different volume fractions:

- The low-stiffness C-S-H phase, to which we refer as C-S-H_a phase [21, 22], has a mean stiffness of E_a = 21.7 ± 2.2 GPa; while the high-stiffness C-S-H phase (the C-S-H_b phase) has a mean stiffness of E_b = 29.4 ± 2.4 GPa. These mean values for the two-types of C-S-H perfectly agree with the stiffness values reported by Acker [20] for C-S-H characterized by C/S ratio (E_a =20 ± 2; E_b = 31 ± 4). This result is truly remarkable in that the reported values of Acker are for a different cementitious material (low w/c-UHPC material), conducted with another indentation apparatus, and by another research team [20]. This finding actually suggests that the determined mean values of the stiffness of the two types of C-S-H are material properties that do not change from one cementitious material to another. They are intrinsic mechanical properties of the material at the micrometer scale.
- After calcium leaching, the residual mean stiffness of the low-stiffness C-S-H_α phase is E_a = 3.0 ± 0.8 GPa (or 14% of its initial value), while the residual mean stiffness of the high-stiffness C-S-H_b phase is E_b = 12.0 ± 1.2 GPa (or 41% of its initial value). That is, the low-stiffness phase is more heavily affected by the chemical degradation than the high-stiffness phase.

The bi-modal structure of the stiffness histogram can suitably be represented by two Gaussian curves, and the area below can be associated with the volume fractions of the two-types of C-S-H. From Fig. 2 it turns out that the volume fraction of the high-stiffness C-S-H_a is roughly 70%, and the one of the low-stiffness C-S-H_b roughly 30%. These values for the volume fraction of the two types of C-S-H almost perfectly coincide with volume fractions provided by advanced physical chemistry models for w/c = 0.5 cementitious materials [25, 26], in which these volume fractions are attributed to low-density and high-density C-S-H. Remarkably, these volume fractions are not affected by calcium leaching (Fig. 2b).

3.2 Hardness measurements

Fig. 4 displays the histograms of hardness measurements of the w/c = 0.5 cement paste, which exhibits similar features as the elasticity histograms, in terms of volume fractions and mean values, particularly in the degraded state. The mean hardness values for the non-degraded state are in very good agreement with the values reported by Acker [20] (H_a = 0.8 ± 0.2 GPa; H_a = 0.9 ± 0.3 GPa), which underscores our proposal that the nanoindentation results provide access to intrinsic material properties at the micrometer range that do not depend on mix proportions. Furthermore, the figures show that the high-density C-S-H_a phase chemically softens much more than the low-density C-S-H_b phase; the first has residual values of hardness of roughly 8% of the initial one, in comparison with 15% for C-S-H_b.

4. DISCUSSION

It has long been argued in cement chemistry that the smallest elementary solid component of cement-based material -that is, the C-S-H- exists in at least a low density and a high density form that can be associated with outer and inner products. The nanoindentation test results on intact and calcium leached materials confirm the existence of these two types of C-S-H and identify their role on the elastic stiffness and hardness of cement-based materials. In other words, nanoindentation confirms, via a mechanics perspective, physical chemistry investigations of the morphology of C-S-H gel formation. While the volume fractions of the two types of C-S-H depend on mix proportions [25, 26, 21], the mean elastic stiffness and hardness values obtained at the micrometer scale do not change from one cement-based material to another; instead they are intrinsic material properties at the micrometer scale. Despite the chemical similarity of C-S-H_a and C-S-H_b, the marked difference between these phases in terms of stiffness and hardness indicates an effect of microstructure (%-porosity).

Furthermore, nanoindentation tests on calcium-leached cementitious materials show that the volume fraction of the two types of C-S-H does not change during calcium leaching, but only the mean stiffness and the mean hardness

values. This is readily understood from the morphology of the two types of C-S-H. The high density C-S-H_b- phase (inner products) degrade much less than the low-density C-S-H_a- phase (outer products) coating it. This phenomenon is more pronounced for the chemical degradation of the stiffness values (chemical damage), than for the one of the hardness values (chemical softening). Ultimately, the scale which is accessible by nanoindentation is the scale where physical chemistry meets mechanics. This finding may well serve as a backbone for the development of new sustainable cement-based materials. These results may lead to the successful optimization of the mix design (particularly the *w/c* ratio), to obtain increased volume fractions of the C-S-H_b- phase and thus cement-based materials with low chemomechanical leaching tendencies [21, 22]

REFERENCES

[1] Brinell, J.A, 'Congrès International des Méthodes d'Essai des Matériaux de Construction', Paris, Tome 2, 83-94 1901.

[2] Tabor, D., 'The Hardness of Metals' (Oxford classical texts in the physical sciences - First published 1951, 2000).

[3] Boussinesq, J., 'Applications des potentiels à l'étude de l'équilibre et du mouvement des solides élastiques', (Gauthier-Villars, 1885).

[4] Hertz, H., 'On the contact of elastic solids (in German), Zeitschrift für die Reine und angewandte Mathematik', English translation in miscellaneous papers (translated by D.E. Jones and G.A. Schott) (1881) **99** 146-62. Macmillan, London, UK, (1986) **92** 156-71.

[5] Sneddon, I., 'The relation between load and penetration in the axisymmetric Boussinesq problem for a punch of arbitrary profile', *International Journal of Engineering Science* **3** (1965) 47.

[6] Doerner, M.F. and Nix, W.D., 'A method for interpreting the data from depth-sensing indentation instruments', *Journal of Material Research* **1** (1986).

[7] Pharr, G.M., Oliver, W.C. and Brotzen F.R., 'On the generality of the relationship among contact stiffness, contact area, and elastic modulus during indentation', *Journal of Material Research* **7** (3) (1992) 613-617.

[8] Giannakopoulos, A.E. and Suresh, S., 'Determination of elastoplastic properties by instrumented sharp indentation', *Scripta Materialia* **40** (10) (1999) 1191-1198.

[9] Dao, M., Chollacoop, N., Van Vliet, K.J., Venkatesh, T.A. and Suresh, S., 'Computational modeling of the forward and reverse problems in instrumented sharp indentation', *Acta Materialia* **49** (19) (2001) 3899-3918.

[10] King, R.B, 'Elastic analysis of some punch problems for a layered medium', *International Journal of Solids and Structures* **23** 1657.

[11] Suresh, S. and Giannakopoulos, A.E., 'Report Inst 2/98', Massachusetts Institute of Technology, 1998.

[12] Suresh, S., Giannakopoulos, A.E. and Alcala, J., 'Spherical indentation of compositionally graded materials: Theory and experiments', *Acta Materialia* **45** (4) (1997) 1307-1321.

[13] Giannakopoulos, A.E. and Larsson, P.L. and Vestergaard, R., 'Analysis of vickers indentation', *International Journal of Solids and Structures* **31** (19) (1994) 2679-2708.

[14] Igarashi, S., Bentur, A. and Mindess, S., 'Characterization of the microstructure and strength of cement paste by microhardness testing', *Advances in Cement Research* **8** (30) (1996) 877-92.

[15] Zhu, W. and Bartos, P.J.M., 'Assessment of interfacial microstructure and bond properties in aged (GRC) using a novel microindentation method', *Cement and Concrete Research* **27** (1997) (11) 1701-1711.

[16] Zhu, W. and Bartos, P.J.M., 'Application of depth-sensing microindentation testing to study of interfacial transition zone in reinforced concrete', *Cement and Concrete Research* **30** (8) (2000) 1299-1304.

[17] Trtik, P., Reeves, C.M. and Bartos, P.J.M., 'Use of focused ion beam (FIB) for advanced interpretation of microindentation test results applied to cementitious composites', *Materials and Structures* **33** (227) (2000) 189-193.

[18] Kholmyansky, M., Kogan, E. and Kovler, K., 'On the hardness determination of fine-grained concrete', *Materials and Structures* **27** (174) (1994) 584-587.

[19] Velez, K., Maximilien, S., Damidot, D., Fantozzi, G. and Sorrentino, F., 'Determination by nanoindentation of elastic modulus and hardness of pure constituents of portland cement clinker', *Cement and Concrete Research* **31** (4) (2001) 555-561.

[20] Acker, P., 'Micromechanical analysis of creep and shrinkage mechanisms', in F.-J. Ulm, Z.P. Bažant, and F.H. Wittmann, editors, 'Creep, Shrinkage and Durability Mechanics of Concrete and other quasi-brittle Materials', Cambridge, MA, August 2001, Elsevier, Oxford, UK.

[21] Constantinides, G. and Ulm, F.-J., 'The effect of two types of C-S-H on the elasticity of cement-based materials: Results from nanoindentation and micromechanical modeling', submitted in *Cement and Concrete Research*, 2002.

[22] Constantinides, G. and Ulm, F.-J., 'The elastic properties of calcium-leached cement pastes and mortars: a multi-scale investigation', MIT CEE Report R02-01, 2002.

[23] Heukamp, F.H., Ulm, F.J. and Germaine, J.T., 'Mechanical properties of calcium-leached cement pastes: triaxial stress states and the influence of the pore pressures', *Cement and Concrete Research* **31** (5) (2001) 767-774.

[24] Ulm, F-J and Coussy, O., 'Mechanics and durability of solids, Volume I: Solid mechanics', MIT and Prentice Hall series on Civil, Environmental and Systems Engineering (Cambridge, MA, 2002).

[25] Tennis, P.D. and Jennings, H.M., 'A model for two types of calcium silicate hydrate in the microstructure of portland cement pastes', *Cement and Concrete Research* **30** (6) (2000) 855-863.

[26] Jennings, H.M., 'A model for the microstructure of calcium silicate hydrate in cement paste', *Cement and Concrete Research* **30** (1) (2000) 101-116.